SUPPLEMENTAL INFORMATION AND METHODS TO "Metformin Interferes With Bile Acid Homeostasis Through The AMPK-FXR Pathway".

A-SUPPLEMENTAL INFORMATION.

Supplemental Figure 1. A) FXR agonist regulation of putative FXR coactivator and corepressor mRNA levels in HepG2 cells. HepG2 cells were treated with 2µM GW4064 for 18 hours and mRNA level corresponding to indicated proteins analyzed by Q-PCR. Expression levels are expressed relative to the basal level (DMSO) set to 1. Med: mediator complex, HATs: histone acetyltransferases, SWI/SNF: SWItch/Sucrose NonFermentable complex, others: other established comodulators. Data represent the mean ± S.E.M. of 3 independent experiments performed with triplicate assays. P values were calculated using the Student's t-test. *: $p<0.05$; **:$p<0.01$.

Supplemental Figure 2. A) Physical interactions of FXR with putative cofactors by GST pulldown. GST, GST-FXR or GST-cofactors fusion proteins were used as baits for $^{[35]}$S-labeled cofactors or full length FXR respectively. Proteins were allowed to interact in the presence of 2µM GW4064 or vehicle [DMSO, (-)] and separated by SDS-PAGE. B) FXR interacts directly with PGC1α but not with Sirt1. GST pull down experiments were carried out using GST-fused full length FXR (GST-FXR), FXR LBD (GST-FXR LBD) or SMRT C-terminus and $^{[35]}$S-labeled Sirt1 or PGC1α as described in Supplemental Figure 1B. C) Sirt1 interacts directly with PGC1α. GST pulldown experiments were carried out as in above using a GST-Sirt1 fusion protein and $^{[35]}$S-labeled PGC1α. SHD: Sirt1 Homology Domain.

Supplemental Figure 3. Subcellular distribution of FXR and AMPKα. HepG2 cells were treated with 2µM GW4064 and/or 1mM AICAR for 2 hours. After being fixed in 4% paraformaldehyde for 20 min at RT, coverslides were incubated with primary and secondary antibodies as indicated. 4',6'-diamidino-2-phenylindole (DAPI) was used to stain DNA.

Supplemental Figure 4. A) FXR target gene expression in HepG2 cells. HepG2 cells were treated with 2µM GW4064 for 18 hours and total RNA was analyzed for its content in mRNA coding for the indicated protein. Target genes are classified according to their functions or properties: Metab. Metabolism, NRs: nuclear receptors, Inflam.: inflammation, Lipoprot.: lipoproteins. B) Kinetics of FXR target gene induction in HepG2 cells. HepG2 cells were treated with 2µM GW4064 and *BSEP*, *FGF19*, *KNG* and *SHP* mRNA levels measured by Q-PCR. Results are expressed relative to the basal level (DMSO, t_0) set to 1. Data represent

the mean ± S.E.M. of 3 independent experiments performed in HepG2 cells were treated 2μM GW4064 and/or 1mM AICAR for 6 hours. Gene expression levels were assessed by RT-QPCR assays. Data represent the mean ± S.E.M. of 3 independent experiments performed in triplicate. P values were calculated by ANOVA followed by a Tukey's post-hoc test. *P < 0.05, **P < 0.01, ***P<0.005. C) FXR target gene expression in HepG2 cells. The expression of fibrinogen beta (FGB) and of the Solute Carrier Organic Anion Transporter (OATP) was assayed by RT-QPCR and quantified as in A).

Supplemental Figure 5. ChIP-Seq profile of *SHP* (*NR0B2*) and *KNG* gene loci. HepG2 cells were treated for 2 hours or not with 2μM GW4064. After formaldehyde crosslinking, chromatin was immunoprecipitated using the indicated antibodies (anti-FXR, anti-RXR, anti-total RNApolII and anti-histone H3K4me3). DNA libraries were prepared and sequenced on a GAIIx Illumina sequencer (36b reads, single end). After data processing using the Cistrome pipeline as described (1;2), peaks were vizualized using the Integrative Genomics Browser [Broad Institute, (3).

Supplemental Figure 6. Biochemical parameters of mice after GW4064 and/or AICAR administration. GW4064 (30mpk daily by gavage in 1% CMC, 1% Tween 80) and/or AICAR (200mpk daily by intraperitoneal injection) were administered to mice (n=6-8) for 5 days. After euthanasia, blood and organs were quickly removed, weighed and snap-frozen. Body mass and plasma concentrations of lipids and glucose were assayed. Results are expressed as the mean ± S.E.M. (n=6-8). P values were calculated using an one-tailed ANOVA followed by a Tukey's post-hoc test.

Supplemental Figure 7. Murine FXR activity is inhibited by AICAR- and metformin. Murine AML12 hepatocyte cells were transfected with the Gal4-tk Luc reporter gene and an expression vector coding for Gal4 DBD fused to full length mFXRα4 (Gal4-mFXRα4). Cells were treated 24 hours after transfection as indicated (2μM GW4064, 1mM metformin or 1mM AICAR), after which luciferase activities were assayed. Values represent the -fold activation over the activity of pGL3-tk Luc alone arbitrarily set to 1, and are the mean ± S.E.M. of 3-5 independent experiments, each performed in triplicate. P values were calculated using a one-tailed ANOVA followed by a Tukey's post-hoc test. *** p<0.005.

Supplemental Figure 8. The mutation of putative AMPK phosphorylation sites does not prevent the AMPK-mediated transcriptional inhibition of hFXRα2. Point mutations were introduced in the human FXRα2 sequence and their effects assessed in a standard one-hybrid assay in HepG2 cells. The left panel indicates the aminoacid numbering

of putative AMPK phosphorylation sites in the mFXRα3 sequence and corresponding residues in the human FXRα2 polypeptide. Results are expressed relative to the FXR transcriptional activity observed in the presence of 2μM GW4064 and set arbitrarily to 100%. Values are the mean ± S.E.M. of 3 independent experiments, each performed in triplicate. P values were calculated using a one-tailed ANOVA followed by a Tukey's post-hoc test. *** p<0.005.

Supplemental Figure 9. mRNA and protein expression knockdown by small interfering RNAs. The efficiency of siRNA pools was assessed by monitoring the level of expression of the targeted mRNA by Q-PCR (A) and of the targeted protein by western blotting (B). Data represent the mean ± S.E.M. of 2 independent experiments performed with triplicate assays. . P values were calculated by ANOVA followed by a Tukey's post-hoc test. *P < 0.05, **P < 0.01, ***P<0.005. B) Western blotting was carried out using HepG2 whole cell extracts and indicated antibodies.

Supplemental Figure 10. AMPK does not target FXR coactivator activity. A) AMPK activation does not alter the intrinsic transcriptional activity of FXR coactivators. HepG2 cells were transfected with the Gal4-tk Luc reporter and Gal4 DBD fused to either flSRC1, flSRC2, flSMRT or flPGC1-α expression vectors. Results are expressed relative to Gal4 control expression vector arbitrarily set to 1. Data represent the mean ± S.E.M. of 3 independent experiments performed with triplicate assays. . P values were calculated by ANOVA followed by a Tukey's post-hoc test. B) AMPK activation prevents coactivator recruitment to FXR in a mammalian 2-hybrid assay. HepG2 cells were transfected with the Gal4-tk Luc reporter gene and a Gal4-DBD fused to human flFXRα2 (Gal4-FXR) without (-) or with an expression vector coding for the receptor interacting domain (RID) from SRC1 or SRC3. Cells were treated for 24 hours after transfection as indicated, after which luciferase activities were assayed. Data represent the mean ± S.E.M. of 3-5 independent experiments performed with triplicate assays. P values were calculated by ANOVA followed by a Tukey's post-hoc test. ***P<0.005.

Supplemental Figure 11. FXR phosphorylation in HepG2 cells. HepG2 cells were transfected with the mFXRα2 expression vector and treated 24 hours later by 2μM GW4064, 2mM AICAR or both for 18 hours. Whole cell extracts were prepared and immunoprecipitated with an anti-FXR antibody. Western blot analysis of immunoprecipitates was carried out using either the anti-phospho FXR antibody (S250P FXR) or a pan-FXR antibody. Numbers indicates the fold increase in phospho-FXR normalized to total FXR content.

Supplemental Figure 12. FXR and RXR binding to the *KNG* promoter FXRE. A) Validation of the specificity of the anti-FXR antibody. Mouse liver from either liver $FXR^{-/-}$ (FXR-/-) or their wild type littermates ($FXR^{+/+}$) were treated with 1% formaldehyde and crosslinked, sonicated chromatin was immunoprecipitated using theSantaCruz H130 FXR antibody. The *Bsep* promoter region or a myoglobin control region were amplified by QPCR and results expressed as the fold enrichment over background (mean ±SEM, n=3, ***:p<0.005). B) FXR and RXR recruitment to the KNG promoter region. HepG2 cells were treated for 2 hours or not with 2μM GW4064 and 250μM resveratrol (Rsv) or 1mM metformin (Met). After formaldehyde crosslinking and chromatin shearing, chromatin was immunoprecipitated using the indicated antibodies (anti-FXR or anti-RXR). Immunoprecipitated DNA was then amplified by PCR using primers specific for the kininogen (KNG) promoter as described in the Material and Methods section. Amplified DNA was analyzed on a 1% agarose gel.

Supplemental Figure 13. The FXR cistrome is not altered upon metformin treatment in mouse liver. Mouse livers were removed and crosslinked with 1% formaldehyde. After cell lysis and chromatin sonication, FXR was immunoprecipitated and associated DNA fragments were used to build DNA libraries which were sequenced on an Illumina HiSeq sequencer (50b reads, single end). After data processing using the Cistrome pipeline as described (1;2) and read numbers were normalized. MACS files were then concatenated to generate a reference list of FXR genomic binding sites. An in-house software was then used to calculate the ratio peak condition1/signal peak condition 2 and plotted as a scatter plot. Amongst > 7,500 FXR binding sites, only 45, 47, 24 and 47 showed fold changes above 3 when comparing chow vs Metformin, chow vs TCA, chow vs TCA+ metformin, and TCA vs TCA+metformin conditions, respectively. B) Shp/Nr0b2 and Bsep/Abcb11 genomic loci were visualized using the Integrative Genomics Browser [Broad Institute, (3)].

Supplemental Figure 14. A-B) Metformin does not affect basal FXR target gene expression in vivo. A) C57Bl6 mice (n=8) were fed a high fat diet for 12 weeks and treated with metformin by gavage (100 mpk/day) for 3 or 10 days. Left panel: *Shp* and *Bsep* mRNA in liver. Gene expression levels were assessed by RT-QPCR assays. Data represent the mean ± S.E.M.. P values were calculated by ANOVA followed by a Tukey's post-hoc test. Right panel: Blood glucose levels in HFD-fed (Control), HFD-fed mice treated or not with metformin for 3 or 10 days. B) Gene expression levels in liver from female obese diabetic (OD) patients treated (OD+Met) or not (OD) with metformin for more than 3 months (3-14 months). BMI ranged from 38 to 47, with age varying from 47 to 62.

Supplemental Figure 15. Biometric parameters of mice after a bile acid load. Mice were fed either a chow diet (Chow), supplemented with 0.5% TCA (TCA), and with or without metformin in drinking water to reach 50-80mpk/day. After euthanasia, organs were quickly removed, weighed and snap-frozen. Organ weights are expressed relative to the total body mass. Results are expressed as the mean ± S.E.M. (n=6-8). P values were calculated using an one-tailed ANOVA followed by a Tukey's post-hoc test. *$p < 0.05$, **$p < 0.01$, *** $p<0.005$.

Supplemental Figure 16. FXR phosphorylation in liver from TCA and/or metformine-challenged mice. Whole cell extracts from mouse liver (n=4) were immunoprecipitated using an anti-FXR antibody and analyzed by western blotting using the anti phospho-S250 FXR antibody (IP:FXR; WB: S250P FXR) or a pan-FXR antibody (IP:FXR; WB: FXR). Bands were quantified using the Genetools software from Syngene (Cambridge, UK) and data are reported as the mean ± SEM in Figure 8D.

Supplemental Figure 17. FXR expression in liver and ileum from liver FXR KO (L*Fxr*$^{-/-}$) mice. *Fxr* expression in liver and ileum from wild type littermates and LFxr$^{-/-}$ mice was quantified by RT-QPCR. *Fxr* expression was set to 1 in wt mice and results expressed relative to this level.

Supplemental Figure 18. Liver injury markers in diabetic patients. Biochemical parameters from 302 obese diabetic patients were analyzed, amongst whom 191 were treated with metformin at usual doses (1.5-2.5 g/day). Average duration of diagnosed diabetes was 7.19±5.66 years, BMI=48.67±8.02; age=46.71±9.60 years; fasting glucose 8.506±3.08; HbA1c=7.73±1.71. A graphic representation of γ-GT concentrations in metformin and non-metformin treated patients is shown.

Supplemental Figure 19. FXR phosphorylation in cholestatic mouse liver. Mice were challenged by ANIT after metformin pre-treatment or not as described in the text. Whole cell extracts from mouse liver (n=6-8) were prepared and immunoprecipitated using an anti-FXR antibody and analyzed by western blotting using the anti phospho-S250 FXR antibody (IP:FXR; WB: S250P FXR) or a pan-FXR antibody (IP:FXR; WB: FXR). Bands were quantified using the Genetools software from Syngene (Cambridge, UK) and data are reported as the mean ± SEM in Figure 10C.

Supplemental Figure 20. FXR/RXR loading at the *BSEP* promoter region in HepG2 cells. A) ChIP-PCR analysis of the *BSEP* promoter. HepG2 cells were treated for 2 hours or

not with 2μM GW4064. After formaldehyde crosslinking and chromatin shearing, chromatin was immunoprecipitated using the indicated antibodies [anti-FXR (Ab FXR), anti-RXR (Ab RXR), anti-histone H3 (Ab H3) and anti-histone H4 (Ab H4). Immunoprecipitated DNA was then amplified by PCR using primers specific for the *BSEP* promoter as described in the Material and Methods section. Amplified DNA was analyzed on a 1% agarose gel. B) ChIP-Seq analysis of the *BSEP* locus. DNA libraries were prepared and sequenced on a GAIIx Illumina sequencer (36b reads, single end). After data processing using the Cistrome pipeline as described (1;2), peaks were vizualized using the Integrative Genomics Browser [Broad Institute, (3)]. The *BSEP* promoter region is indicated in a blue box.

Supplemental Figure 21. FXR phosphorylation at low (1mM) and high (25mM) glucose concentrations. HEK cells were transfected with an expression vector coding for mFXRα3. Forty eight hours after transfection, whole cell extracts were prepared and immunoprecipitated with 3 μg of anti-FXR antibody (Abcam). Immunoprecipitates were analyzed by western blotting using the anti phospho S250 antibody.

B- SUPPLEMENTAL METHODS

Materials.

Resveratrol, DTT, sodium dodecyl sulfate (SDS), dimethyl sulfoxide (DMSO) and metformin were purchased from Sigma Chemicals (St. Louis, USA). GW4064 was a kind gift from Dr D. Hum (Genfit SA, Loos, France). Dulbecco's modified Eagle medium (DMEM), fetal bovine serum (FBS), sodium pyruvate, trypsin, non-essential amino acids (NEAA), and streptomycin/penicillin were from Gibco-BRL (Carlsbad, USA). Charcoal/dextran-treated fetal bovine serum (CD-FBS) was prepared before use. Purified recombinant AMPK was from Cell Signaling Technology (Danvers, USA), and purified His_6-tagged FXR from Active Motif (Carlsbad, USA).

Plasmids.

GST-FXR was obtained by inserting the human *FXRα2* coding sequence (472 amino acids) in frame with GST into a pGEX2T backbone. Similarly, the GST-FXR LBD vector was build by inserting in frame the *FXRα2* cDNA fragment encoding for the C terminal amino acids from residue 214 to 472. FXR mutants were generated by site-directed mutagenesis (QuikChange, Stratagene).

The GST-SRC1, GST-SRC2, GST-SMRT, GST-RIP140, GST-PGC1α, GST-pCAF, GST-p300, GST-CBP, GST-BAF57, GST-BAF60c1, GST-BAF60c2, GST-BAF250 expression vectors

have been described in (4).

The Gal4, Gal4-mFXRα3, Gal4-hFXRα2, Gal4-hRXRα, Gal4-mRXRα, Gal4-hLXRα, Gal4-hLXRβ are pSG24-based vectors and express full length receptors fused to the Gal4 DNA binding domain at their C-terminus. pGal4-tk Luc has been described elsewhere (5). pGL3-tk Luc (pGL3 promoter, Promega) was used as a recipient vector for the insertion of triplicate copies of the FXRE from the human SHP, FGF19 and kininogen promoters to generate pSHP-tk Luc, pFGF19-tk Luc and pKini-tk Luc. pcDNA3-hRXRα and pcDNA3-hFXRα2 were obtained by subcloning of the appropriate cDNA into the pcDNA3 backbone (Invitrogen). pCMV6-AMPKα and AMPKγ expression vectors were from Origene. All sequences are available upon request.

Antibodies and immunoprecipitations.

Anti-panFXR antibodies were purchased from R&D Systems (PP-A9033A-00) or from Santa Cruz Biotech. (H-130), the anti-PGC-1α from Santa Cruz Biotech.Inc. (sc-13067), the anti-Sirt1 (07-131) and anti-phospho Serine (4A4) antibodies from Upstate/Millipore, the anti phospho(T172) AMPKα (40H9, #2535) and anti AMPKα1/2 (#2532) , β2 (#4148) or γ2 (#2536) were from Cell Signaling Technology. The anti phospho S250 antibody was raised in rabbits against a synthetic RDLRQVT(pS)TTKFC peptide coupled to KLH (Proteogenix, Schiltigheim, France).

(Co)immunoprecipitation assays were carried out using the anti-FXR antibody from Abcam (ab28676) and the Magnetic crosslink IP/CoIP kit (Pierce) as recommended by the manufacturer. Immunoprecipitated material was detected using the indicated primary antibody and HRP-conjugated anti-rabbit or anti-mouse IgG (Sigma).

Cell culture and transient transfections.

The human hepatocellular carcinoma cell line HepG2 was obtained from ATCC. HepG2 cells were grown in 150 mm cell culture plates in DMEM supplemented with 10% FBS, 1 mM NEAA and 1% penicillin/streptomycin in a humidified incubator with 5% CO_2 at 37°C. 25×10^4 HepG2 cells were seeded on 6-well plates and incubated under standard conditions for 24 hours. The medium was replaced with serum- and antibiotic-free DMEM (2.5 mL) with the Lipofectamine® 2000 mix. Two hours later, the medium was replaced with DMEM supplemented with 10% FBS, NEAA and antibiotics. Cells were incubated for 24 hours and treated as indicated in the figure legends. AML-12 mouse hepatocytes were grown according to ATCC recommendations (1:1 vol:vol of DMEM and Ham's F12 medium supplemented with 5 µg/mL insulin, 5 µg/mL transferrin, 5 ng/mL selenium, and 100nM dexamethasone, 10% FBS). Caco2/TC7 cells were maintained in DMEM supplemented with Glutamax (Gibco-BRL), 20% SVF, 1% NEAA and 1% penicillin/streptomycin in a humidified incubator with 10% CO_2

at 37 °C. Cells were seeded on inserts at $1x10^4/cm^2$ and grown for 1 week in complete medium. The apical side was then fed with DMEM supplemented with NEAA and antibiotics, and the basolateral medium was fully supplemented DMEM. Cells were further cultured for 3 weeks and treated as detailed in the text. All experiments were performed in triplicate.

AML12 cells overexpressing the GFP-mFXRα1 fusion protein were generated by transducing AML12 cells with lentiviral particles generated with the TET-inducible "all-in-one" lentiviral expression vector (Sirion Biotech, Martinsried, Germany) and further selected using puromycin. Clones were then selected on the basis of their ability t express detectable levels of GFP-FXR after induction by doxycyclin at 2.5µg/mL for 24 hours.

GST pulldowns.

Immobilized GST fusion proteins were incubated in GST-binding buffer consisting of 20 mM Tris-HCl, pH 7.9, 0.2 mM EDTA, 0.1% Nonidet P-40 (NP-40), 0.5 mM PMSF, 1 mM DTT, protease inhibitors (Sigma), containing 1 mg/mL BSA and 100 mM KCl. Immobilized proteins on beads (20µg) were incubated at 4°C for 6-10 hours with 2-6 mg of HepG2 extract in the presence or absence of 1µM GW4064; or 2 µg of GST-fusion proteins on beads were incubated at 4°C for 4 hours in the presence or absence of 1µM GW4064 with *in vitro* translated proteins (TNT-coupled reticulocyte lysate, Promega) with $^{[35]}$S-methionine (GE Healthcare) following the manufacturer's instructions. After three washes with GST-binding buffer supplemented with 150 mM KCl and 0.3% NP-40, samples were resolved by SDS-PAGE, and analyzed either by silver nitrate or colloidal blue staining, or by autoradiography followed by quantification with a Storm 860 phosphorimager (Molecular Dynamics).

Recombinant human FXR purification.

m*FXRα3* cDNA was cloned in pET-52 3C/LIC (Novagen) and expressed as an N-terminally Strep•Tag II-, C-terminally His-tagged recombinant protein in BL21(DE3)pLys bacteria (Novagen). FXR was produced after induction by 1 mM IPTG and purified using the His-select nickel affinity gel (Sigma) to ca. 30-50% purity.

Identification of phosphorylated aminoacids by mass spectrometry.

In gel digestion

In gel digestion was performed with an automated protein digestion system, MassPrep Station (Waters, Milford, USA). The gel bands were washed twice with 50 µL of 25 mM ammonium hydrogen carbonate (NH_4HCO_3) and 50 µL of acetonitrile. Cysteine residues were reduced with 50 µL of 10 mM dithiothreitol at 57°C and alkylated with 50 µL of 55 mM iodoacetamide. After dehydration with acetonitrile,

proteins were cleaved in-gel with 20 µL of 12.5 ng/µL of modified porcine trypsin (Promega, Madison, WI, USA) in 25 mM NH_4HCO_3, 20 µL of 12.5 ng/µL chymotrypsin (Promega, Madison, WI, USA) in 25 mM NH_4HCO_3, 20 µl of 10 ng/µL of aspN (Promega, Madison, WI, USA) in 25 mM NH_4HCO_3, and 20 µL of 20 ng/µL of pepsin (Promega, Madison, WI, USA) in HCl 0.04N. The digestion was performed overnight at room temperature for trypsin and chymotrypsin, 2h at 37°C for pepsin digestion and 5h at 37°C for aspN digestion. The generated peptides were extracted with 40 µL of 60% acetonitrile in 0.1% formic acid. Acetonitrile was evaporated under vacuum before nanoLC-MS/MS analysis.

NanoLC-MS/MS analysis

NanoLC-MS/MS analysis was performed on a nanoLC-IT-MS system and on a nanoLC-QTOF-MS system. The nanoLC-IT-MS system was composed of the Agilent 1200 series nanoLC-Chip system (Agilent Technologies, Palo Alto, USA) coupled to the amaZon ion trap (Bruker Daltonics GmbH, Bremen, Germany). The system was fully controlled by HyStar 3.2 and trapControl 7.0 (Bruker Daltonics, Bremen, Germany).

The chip was composed of a Zorbax 300SB-C18 (150 mm × 75 m, with a 5 µm particle size) analytical column and a Zorbax 300SB-C18 (40 nL, 5 µm) enrichment column. The solvent system consisted of 2% acetonitrile, 0.1% formic acid in water (solvent A) and 2% water, 0.1% formic acid in acetonitrile (solvent B). 4 µL of sample were loaded into the enrichment column at a flow rate set to 3.75µL/min with solvent A. Elution of the peptides was performed at a flow rate of 300 nL/min with an 8-40% linear gradient of solvent B in 35 minutes.

For tandem MS experiments, the system was operated in Data-Dependent-Acquisition (DDA) mode with automatic switching between MS and MS/MS. The voltage applied to the capillary cap was optimized to -1850V. The MS scanning was performed in the standard enhanced resolution mode at a scan rate of 8100 m/z per second. The mass range was 250-1500 m/z. The Ion Charge Control was 200,000 and the maximum accumulation time was 200 msec. A total of 2 scans was averaged to obtain a MS spectrum and the rolling average was 1. The six most abundant precursor ions with an isolation width of 4 m/z were selected on each MS spectrum for further isolation and fragmentation by CID and ETD. The MS/MS scanning was performed in the ultrascan mode with a scan rate of 32 500 m/z per second. The mass range was 100-2000 m/z. The Ion Charge Control was 300,000. A total of 2 scans was averaged to obtain an MS/MS spectrum.

Mass data collected during analysis were processed and converted into .mgf files using DataAnalysis 4.0 (Bruker Daltonics GmbH, Bremen, Germany). A maximum of 1700 compounds was detected with an intensity threshold of 150,000. A charge

deconvolution was applied on the MS full scan and the MS/MS spectra with an abundance cutoff of 5% and 2% respectively and with a maximum charge state of 3 and 2 respectively. The nanoLC-QTOF-MS system was composed of the nanoACQUITY Ultra-Performance-LC (Waters Corporation, Milford, USA) coupled to the SynaptTM High Definition Mass SpectrometerTM (Waters Corporation, Milford, USA). The system was fully controlled by MassLynx 4.1 SCN639 (Waters Corporation, Milford, USA). The nanoLC system was composed of ACQUITY UPLC® BEH130 C18 column (250 mm x 75 µm with a 1.7 µm particle size, Waters Corporation, Milford, USA) and a Symmetry C18 precolumn (20 mm × 180 µm with a 5 µm particle size, Waters Corporation, Milford, USA). The solvent system consisted of 0.1% formic acid in water (solvent A) and 0.1% formic acid in acetonitrile (solvent B). 4 µL of sample were loaded into the enrichment column during 3 min at 5 µL/min with 99% of solvent A and 1% of solvent B. Elution of the peptides was performed at a flow rate of 300 nL/min with a 8-35% linear gradient of solvent B in 35 minutes.

The tandem mass spectrometer was equipped with a Z-spray ion source and a lock mass system. The capillary voltage was set at 3.2 kV and the cone voltage at 35 V. Mass calibration of the TOF was achieved using fragment ions from Glu-fibrino-peptide B on the [50;2000] m/z range. Online correction of this calibration was performed with Glu-fibrino-peptide B as the lock-mass. The ion (M+2H)2+ at m/z 785.842 was used to calibrate MS data and the fragment ion (M+H)+ at m/z 684.347 was used to calibrate MS/MS data during the analysis. The system was operated in Data-Dependent-Acquisition (DDA) mode with automatic switching between MS (0.5 s/scan on m/z range [150;1700]) and MS/MS modes (0.5 s/scan on m/z range [50;2000]). The two most abundant peptides (intensity threshold 20 counts/s), preferably doubly and triply charged ions, were selected on each MS spectrum for further isolation and CID fragmentation using collision energy profile. Fragmentation was performed using argon as the collision gas.

Mass data collected during analysis were processed and converted into .pkl files using ProteinLynx Global Server 2.3 (Waters Corporation, Milford, USA). Normal background subtraction type was used for both MS and MS/MS with 5% threshold and polynomial correction of order 5. Smoothing was performed on MS/MS spectra (Savitsky-Golay, 2 iterations, window of 3 channels). Deisotoping was applied for both MS (medium desisotoping) and MS/MS (fast deisotoping).

Protein identification

MS/MS data were interpreted using two search engines, MASCOT 2.4.0 (Matrix Science, London, UK) and OMSSA 2.1.7 (http://msda.unistra.fr) against UniProtKB/SwissProt (version 2012_12, 538,585 sequences). The research was

carried out in all species. No enzyme was specified. Spectra from nanoLC-QTOF-MS were searched with a mass tolerance of 15 ppm for MS and 0.05 Da for MS/MS data and spectra from nanoLC-IT-MS were searched with a mass tolerance of 0.3 Da in MS and MS/MS modes. Carbamidomethylation of cysteine residues, oxidation of methionine residues and phosphorylation of serine or threonine residue were specified as variable modifications. Protein identifications were validated with at least two peptides with Mascot ion score above 30.

RNA extraction, cDNA synthesis, and real-time RT-PCR.

Total RNA was extracted using RNEasy (Qiagen) according to the manufacturer's instructions. Quantification and purity of RNA were checked using a Nanodrop device (Nanodrop Technologies, Wilmington, DE). DNase I-treated total RNA was reverse-transcribed using the High-Capacity cDNA archive kit (Applied Biosystems, Foster City, CA, USA) following the manufacturer's recommendations. Genes were analyzed using TaqMan® Gene Expression Assays. 250 ng of cDNA were used in a total reaction mixture of 15 µL Taq Master Mix (2×). qRT-PCR conditions were : step 1, 95°C for 10 min; step 2, 40 cycles of 15 sec at 95°C and 60°C for 60 sec. All samples were analyzed in duplicate, for at least three independent experiments. PCR amplifications were performed using the ABI Prism 7500 Sequence Detection System (Applied Biosystems). Relative gene expression was calculated by the ΔΔCt method. Final results were expressed as the fold difference in gene expression normalized to 18S rRNA and relative to control conditions.

Chromatin immunoprecipitation assays.

ChIP assays were performed as described previously (6). 200µg of sheared, crosslinked chromatin was immunoprecipitated with either anti-FXR (H-130, Santa Cruz BioTechnology, USA), anti-AMPK or anti-RNA polymerase II antibody (N–20, Santa Cruz BioTechnology). Promoter regions were amplified by semi-quantitative PCR with the following set of primers: KNG: (5' end) GGACTCCTGGAACTCACTG, (3' end) AGGCAACTAGCGTCTGGCAGCA; *BSEP*: (5' end) TTTCCCAAGCACACTCTGTGTTT, (3' end) CCATTATTTCCTCTGGCTTCCTC; *FGF19* (5' end)TCTCCCAAAGGACAAGCCA, (3' end) GAACATTCATAGTCCACGGG; SHP (5' end) GCTGGCTTCCTGGCTTAGC, (3' end)CACTTGAGTCATCTGATAAG.

Biochemical assays.

Cholesterol, glucose, triglycerides, BA, ALT and AST plasma levels were determined as described in (7). Fecal bile salts were determined by gas chromatography as described by Hulzebos et al., 2001 (8).

Liver histology.

Liver lobes were fixed in 5% formaldehyde and embedded in paraffin. Total lobe sections were used for H&E staining and observed under a Leica DMI6000B microscope. Cumulative lesion areas were measured for each mouse (n=6-8) and normalized to the total slice area using the Metamorph software (Molecular Devices). RNAs were extracted as described above.

Statistical methods.

Raw data were processed using GraphPad Prism v5.0. Results are expressed as mean±S.E.M. and groups were compared using either a t-test or one-way ANOVA followed by a Tukey's post hoc test. p values are indicated in the legends to figures.

Reference List

1. Serandour,A.A., Avner,S., Percevault,F., Demay,F., Bizot,M., Lucchetti-Miganeh,C., Barloy-Hubler,F., Brown,M., Lupien,M., Metivier,R. et al 2011. Epigenetic switch involved in activation of pioneer factor FOXA1-dependent enhancers. *Genome Res.* **21**:555-565.

2. Serandour,A.A., Avner,S., Oger,F., Bizot,M.P.F.L.-M.C.P.G., Gheeraert,C., Barloy-Hubler,F., Le Péron,C., Madigou,T., Durand,E., Froguel,P. et al 2012. *Dynamic hydroxymethylation of DNA marks differentiation-driven enhancers.* 8255-8265.

3. Robinson,J.T., Thorvaldsdottir,H., Winckler,W., Guttman,M., Lander,E.S., Getz,G., and Mesirov,J.P. 2011. Integrative genomics viewer. *Nat. Biotechnol.* **29**:24-26.

4. Flajollet,S., Lefebvre,B., Cudejko,C., Staels,B., and Lefebvre,P. 2007. The core component of the mammalian SWI/SNF complex SMARCD3/BAF60c is a coactivator for the nuclear retinoic acid receptor. *Mol Cell Endocrinol* **270**:23-32.

5. Depoix,C., Delmotte,M.H., Formstecher,P., and Lefebvre,P. 2001. Control of retinoic acid receptor heterodimerization by ligand-induced structural transitions. a novel mechanism of action for retinoid antagonists. *J. Biol. Chem.* **276**:9452-9459.

6. Flajollet,S., Lefebvre,B., Rachez,C., and Lefebvre,P. 2006. Distinct Roles of the Steroid Receptor Coactivator 1 and of MED1 in Retinoid-induced Transcription and Cellular Differentiation. *J. Biol. Chem.* **281**:20338-20348.

7. Prawitt,J., Abdelkarim,M., Stroeve,J.H., Popescu,I., Duez,H., Velagapudi,V.R., Dumont,J., Bouchaert,E., van Dijk,T.H., Lucas,A. et al 2011. Farnesoid X receptor deficiency improves glucose homeostasis in mouse models of obesity. *Diabetes* **60** :1861-1871.

8. Hulzebos,C.V., Renfurm,L., Bandsma,R.H., Verkade,H.J., Boer,T., Boverhof,R., Tanaka,H., Mierau,I., Sauer,P.J., Kuipers,F. et al 2001. Measurement of parameters of cholic acid kinetics in plasma using a microscale stable isotope dilution technique: application to rodents and humans. *J. Lipid Res.* **42**:1923-1929.

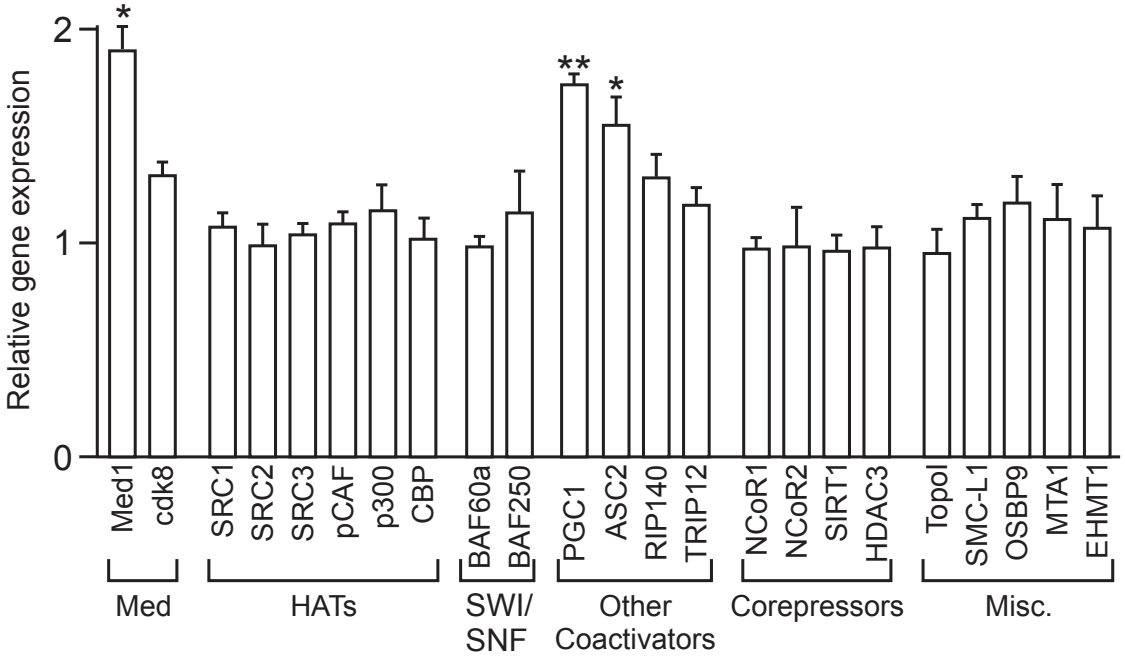

Supplemental Figure 1 - Lien et al.

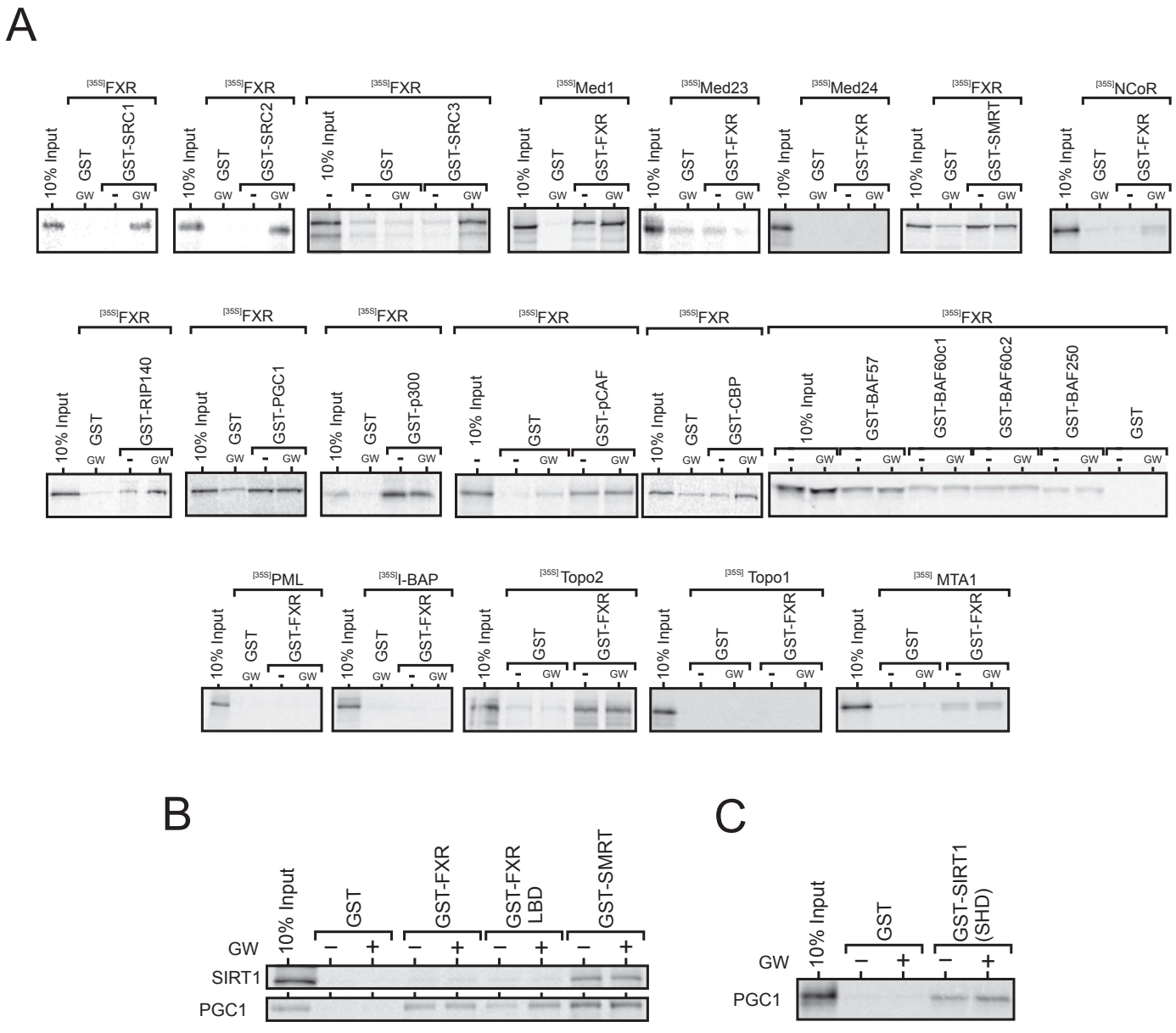

Supplemental Figure 2 - Lien et al.

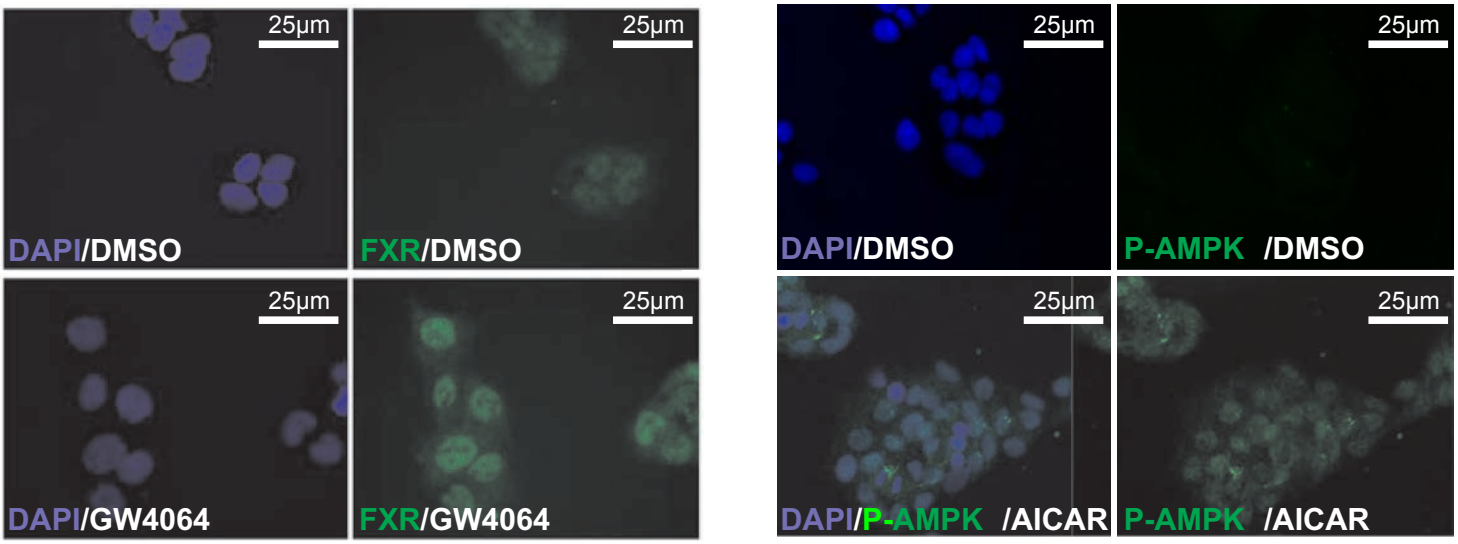

Supplemental Figure 3 - Lien et al.

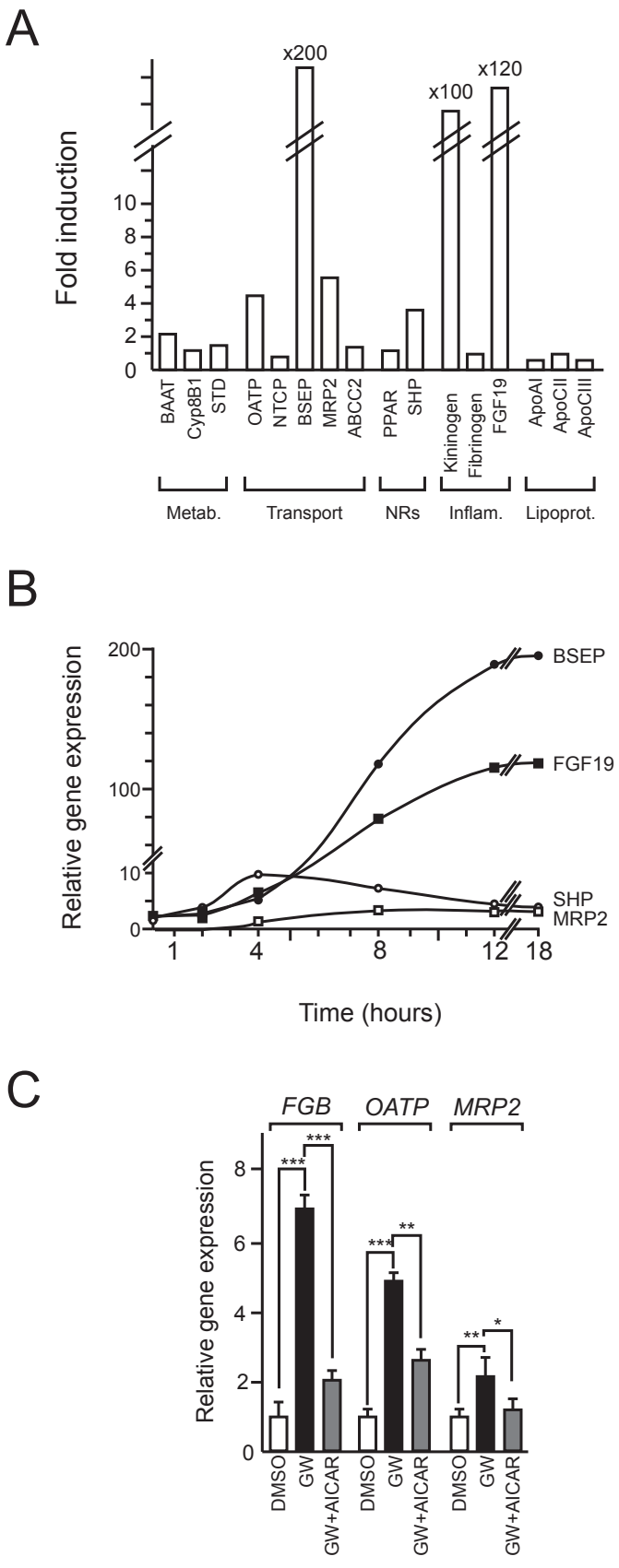

Supplemental Figure 4 - Lien et al.

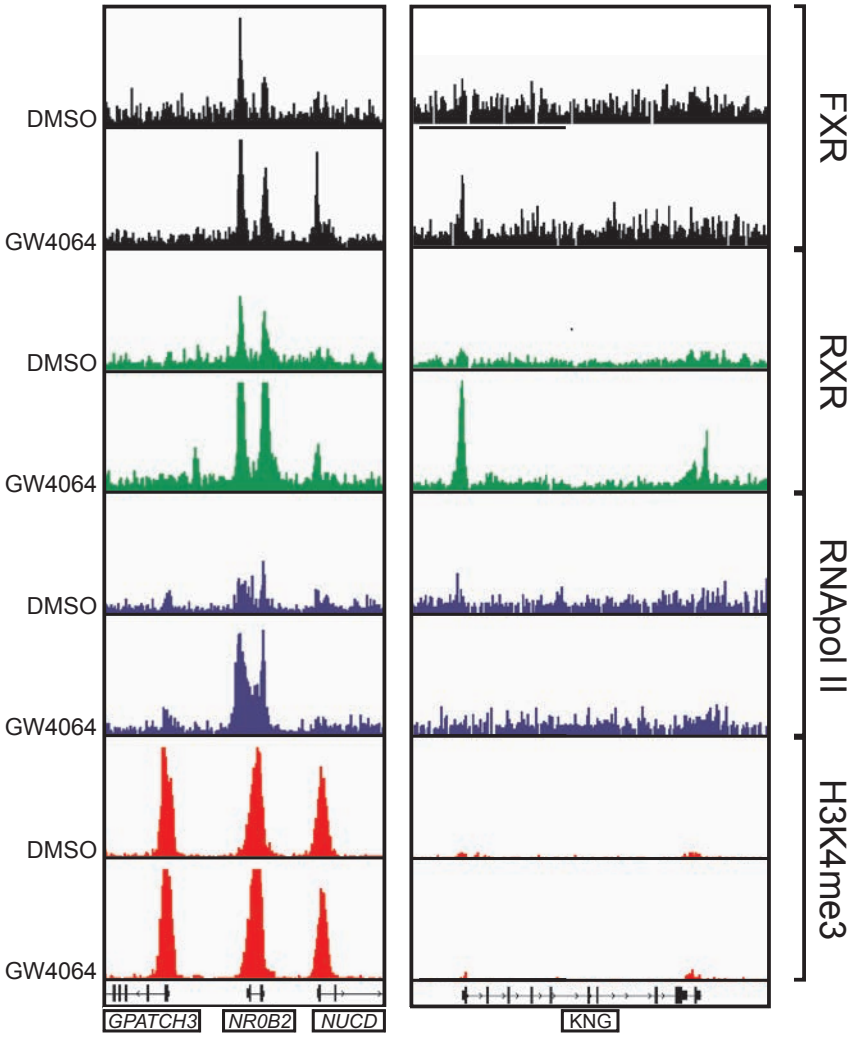

Supplemental Figure 5 - Lien et al.

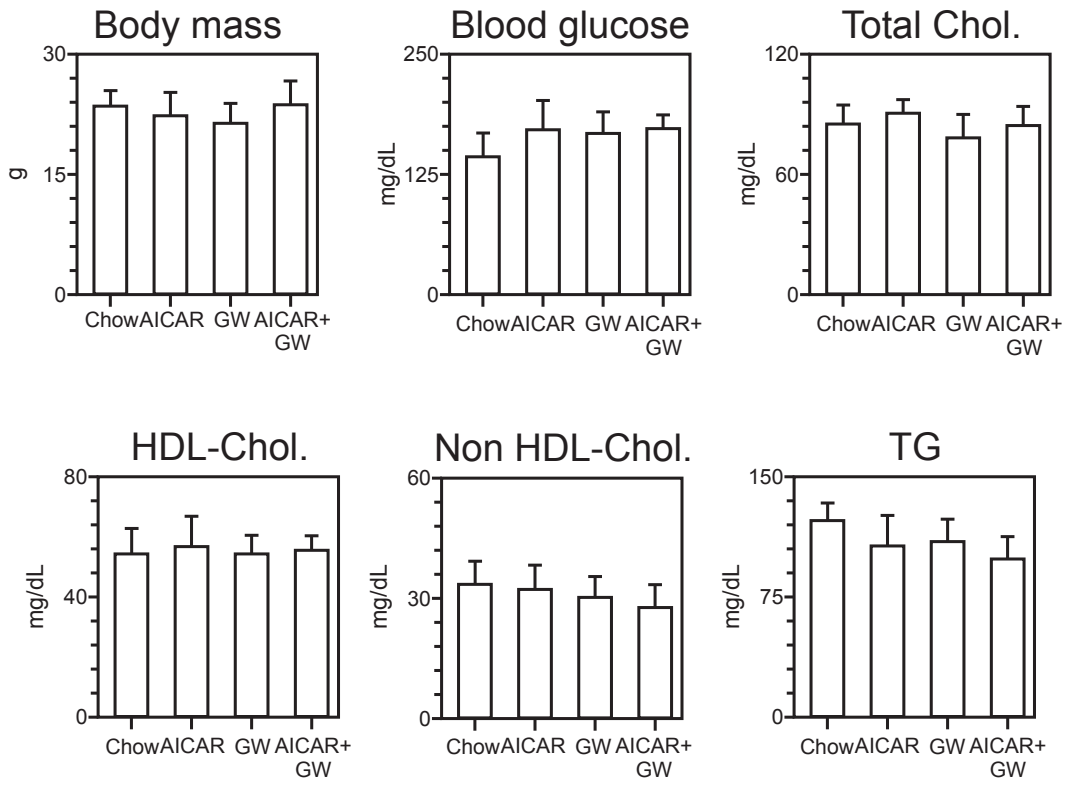

Supplemental Figure 6- Lien et al.

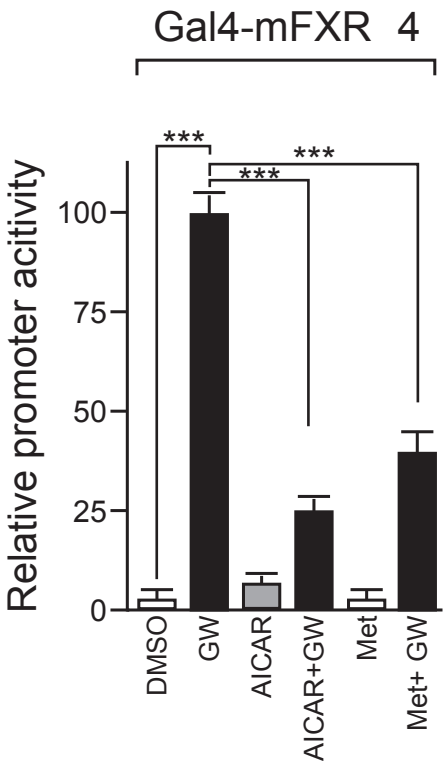

Supplemental Figure 7 - Lien et al.

mFXR 3:	hFXR 2:
S72	S62
S75	S65
S128	S117
T167	T156
S250	**S234**
F254	S238

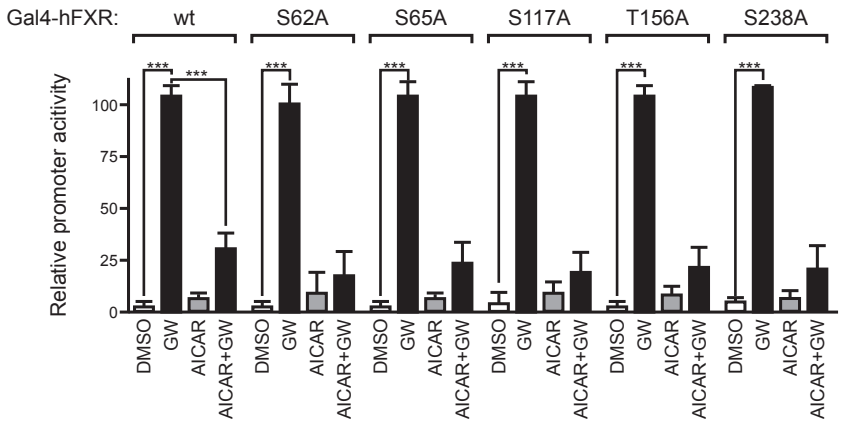

Supplemental Figure 8 - Lien et al.

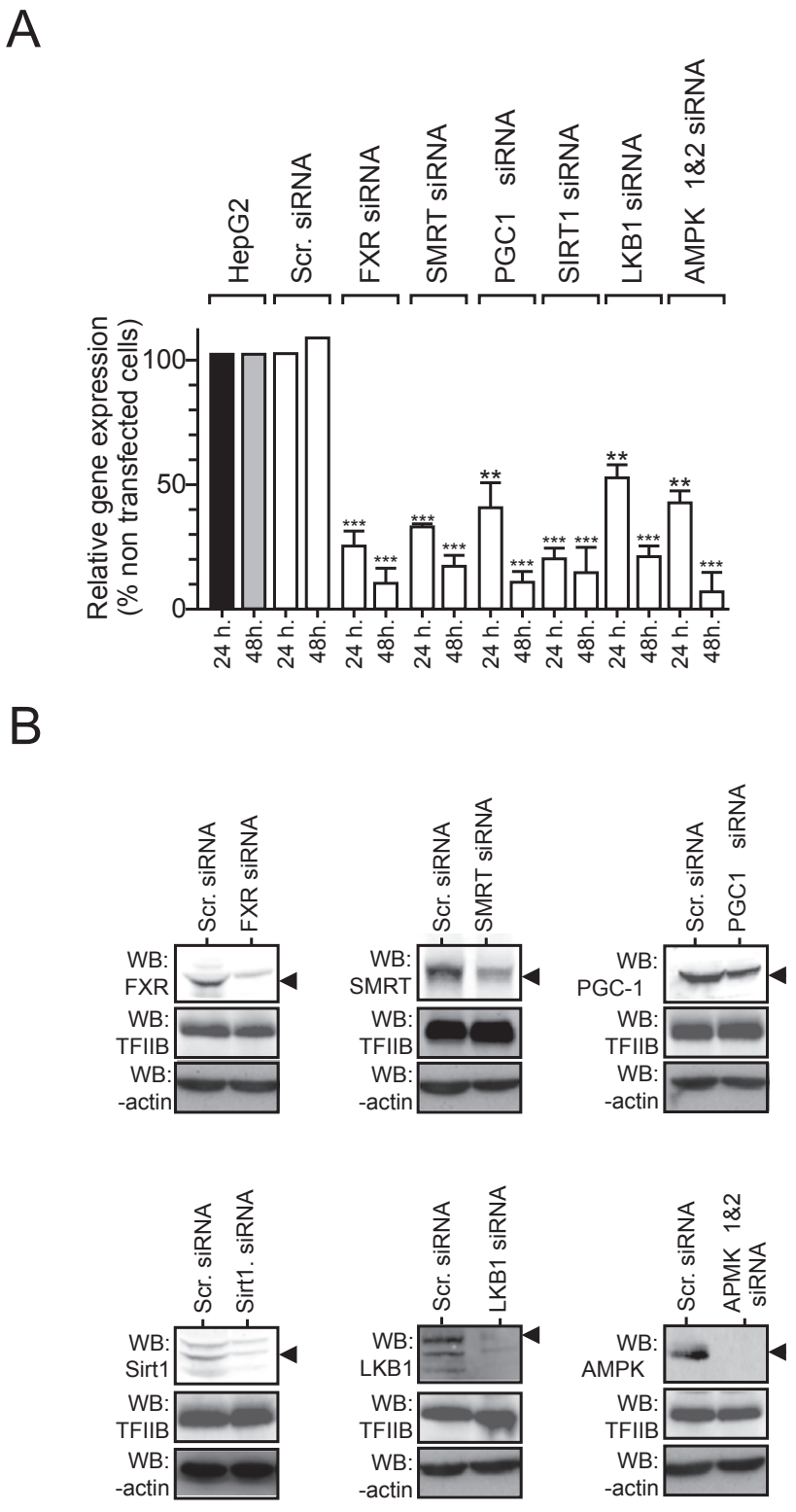

Supplemental Figure 9 - Lien et al.

A

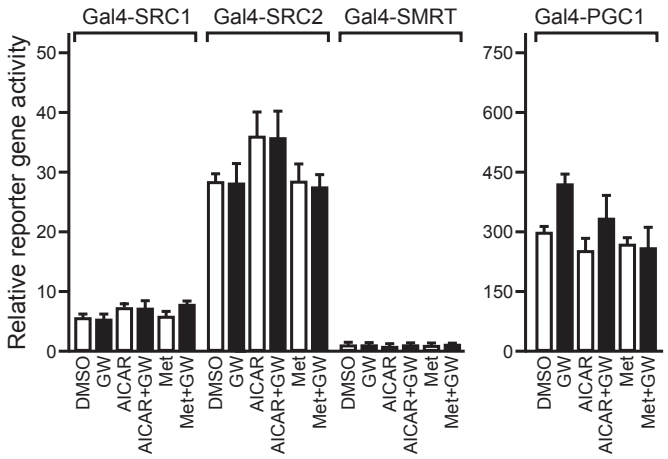

B

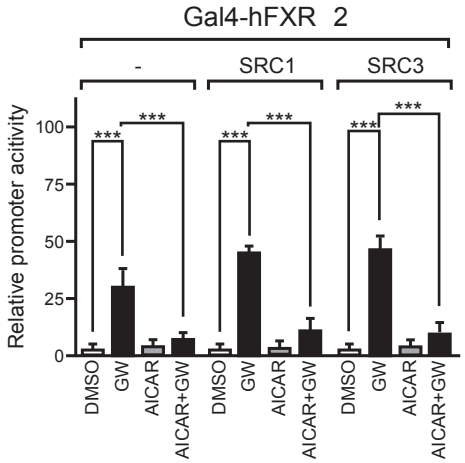

Supplemental Figure 10- Lien et al.

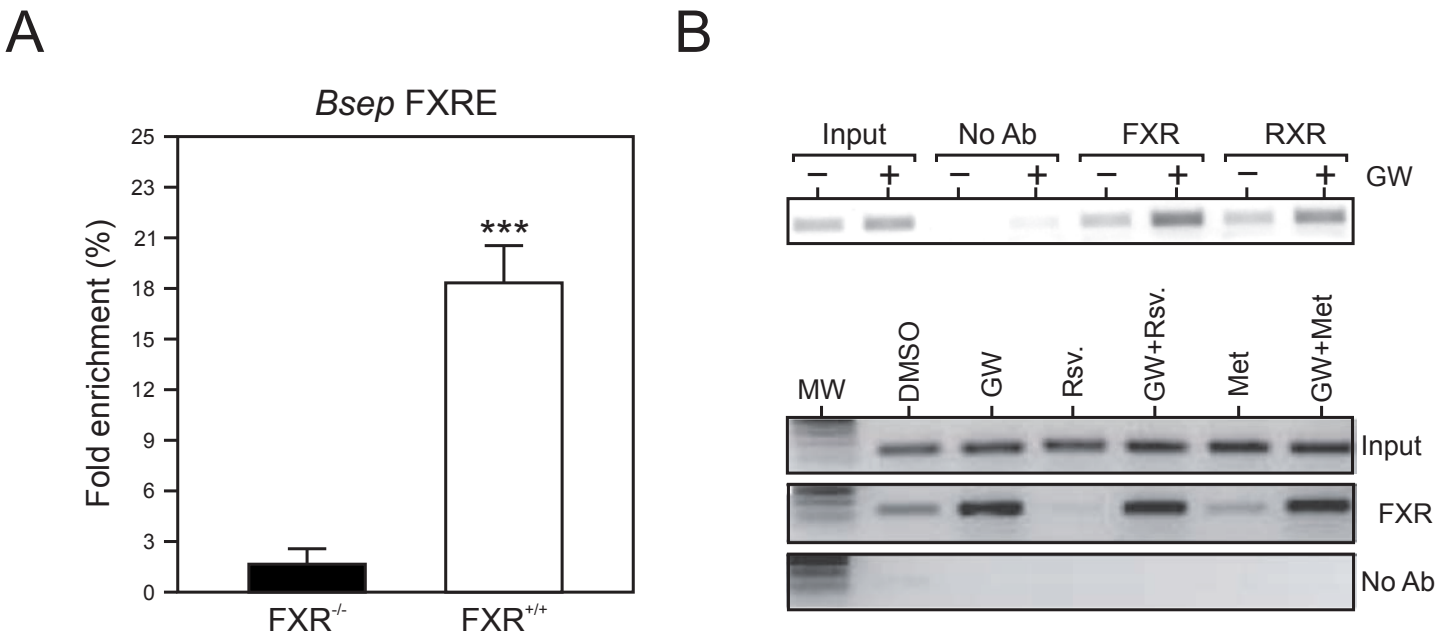

Supplemental Figure 11 - Lien et al.

A

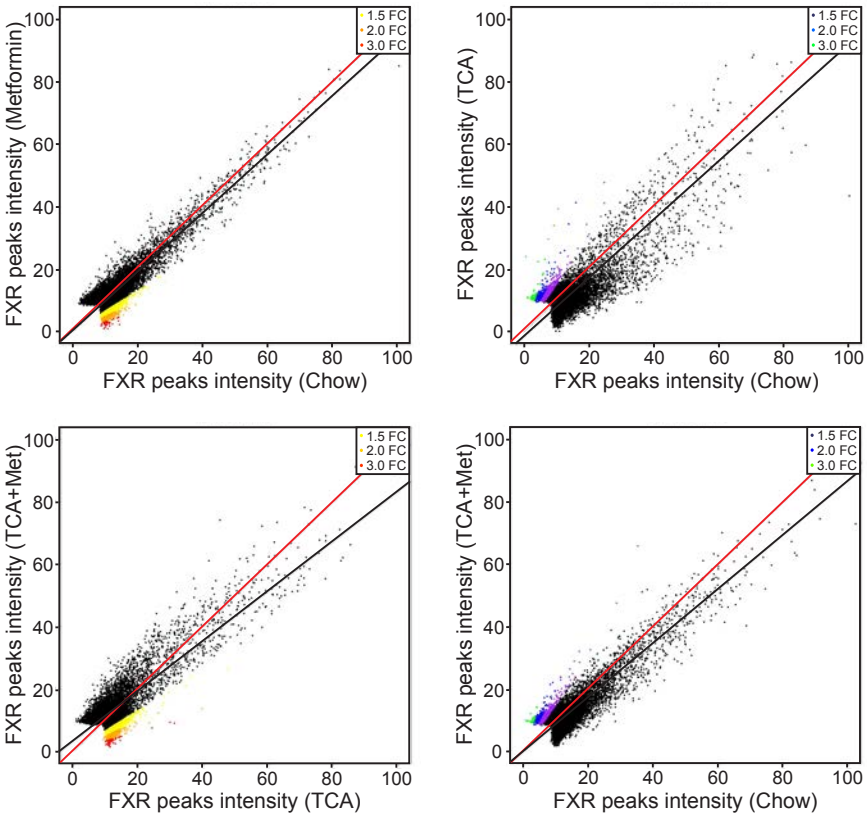

B

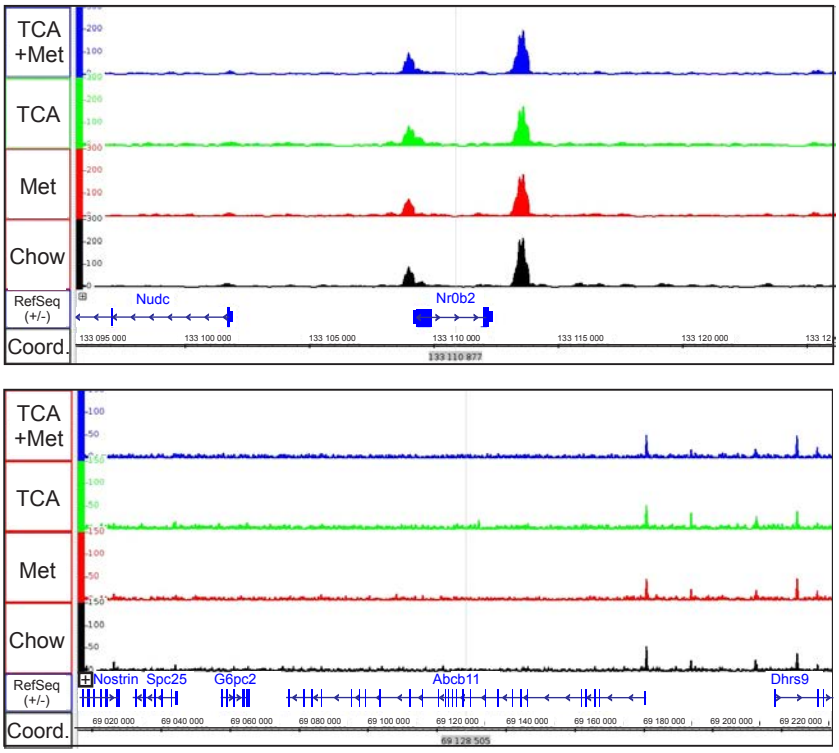

Supplemental Figure 12- Lien et al.

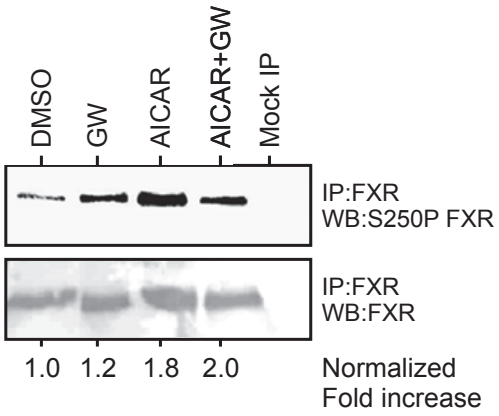

Supplemental Figure 13 - Lien et al.

A-High Fat Diet-fed mice

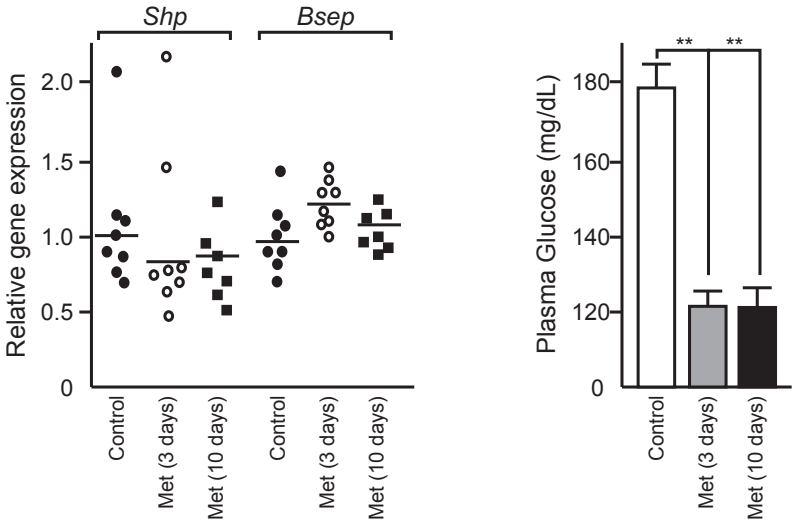

B-Diabetic patients

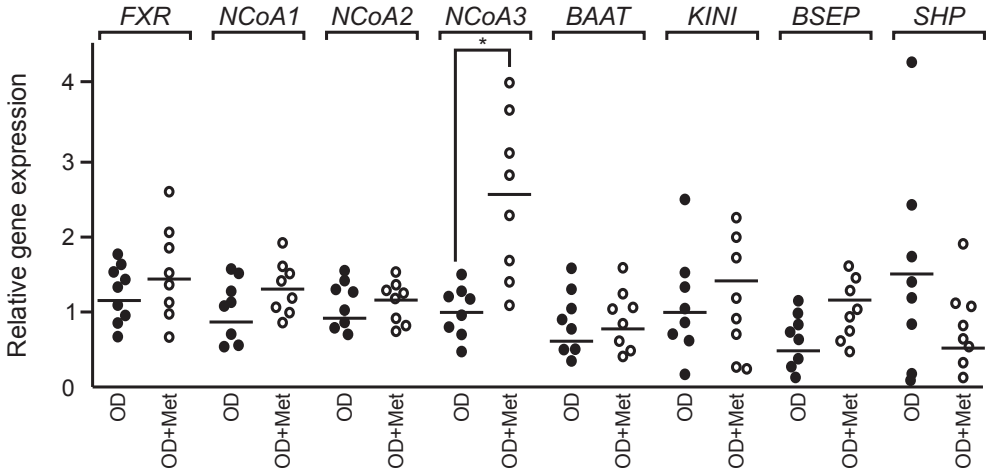

Supplemental Figure 14- Lien et al.

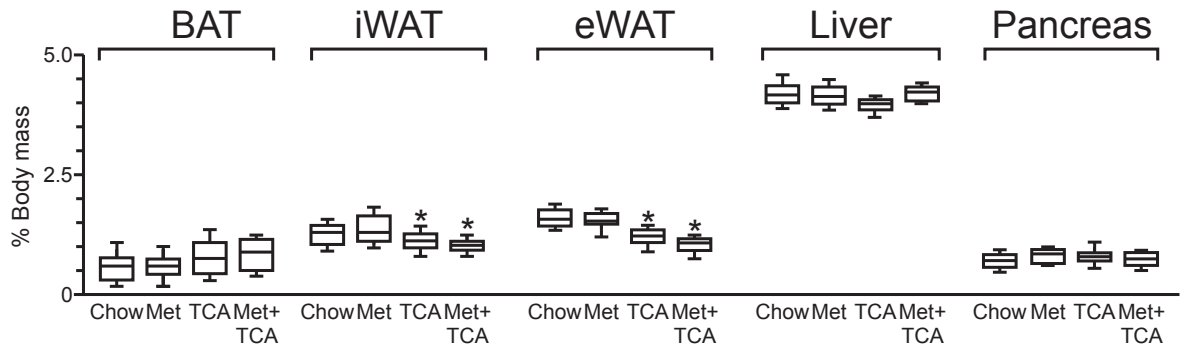

Supplemental Figure 15- Lien et al.

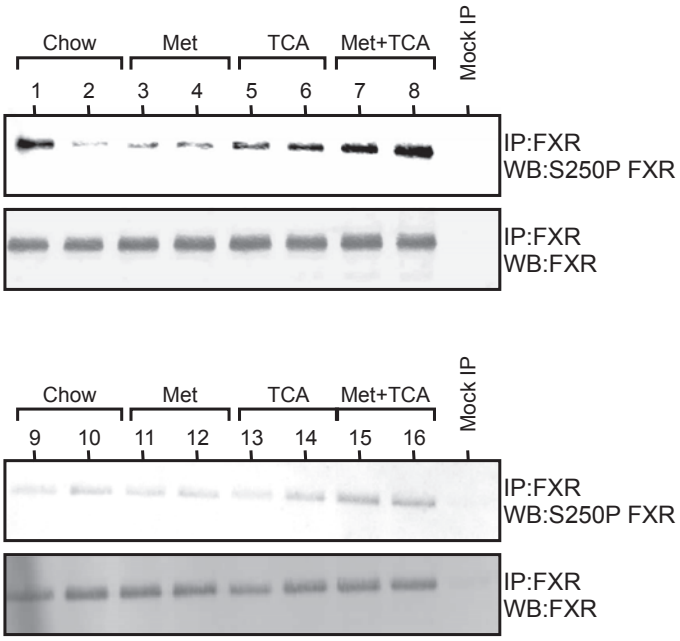

Supplemental Figure 16- Lien et al.

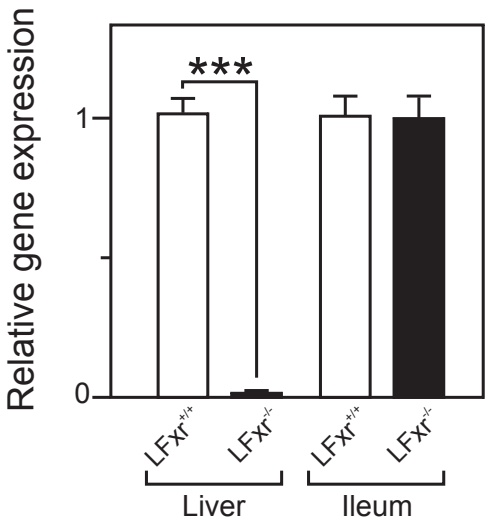

Supplemental Figure 17- Lien et al.

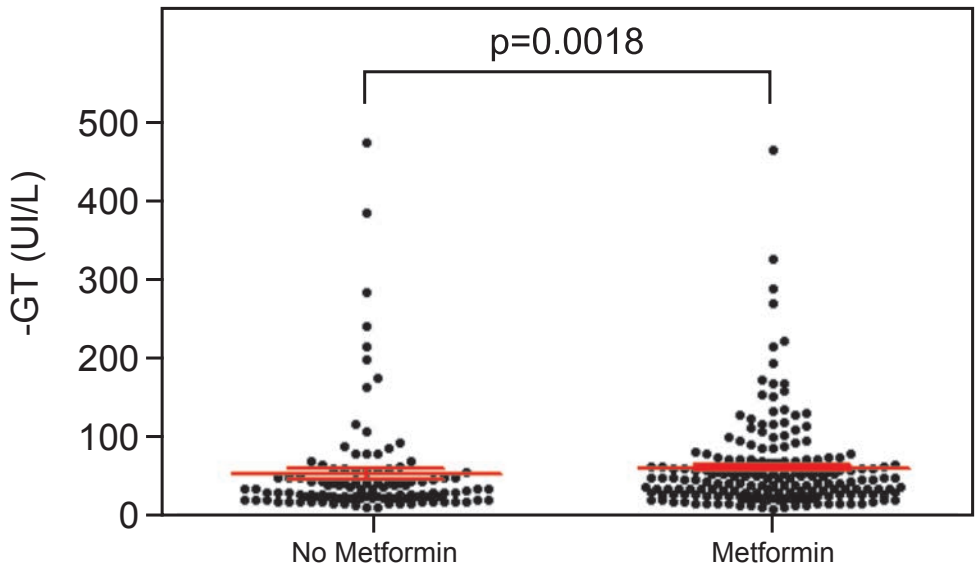

Supplemental Figure 18- Lien et al.

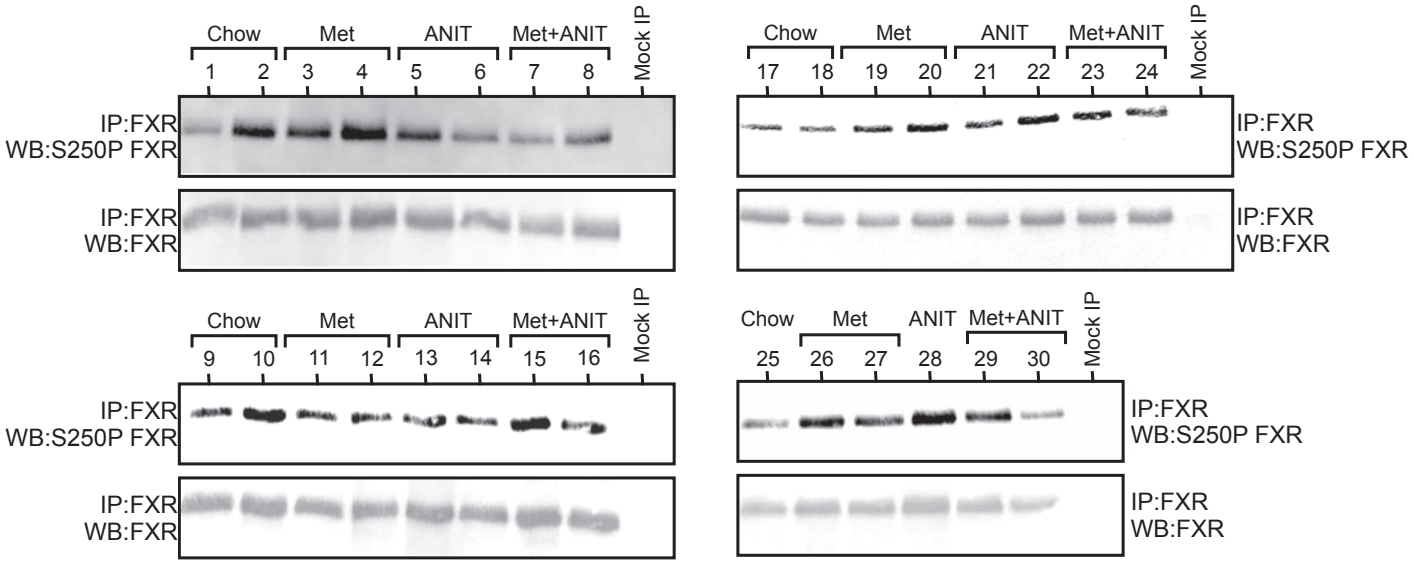

Supplemental Figure 19- Lien et al.

A

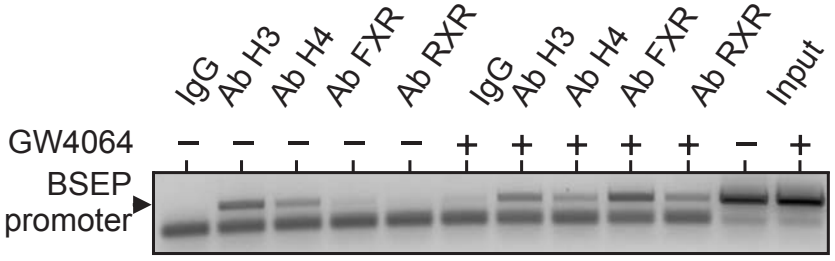

B

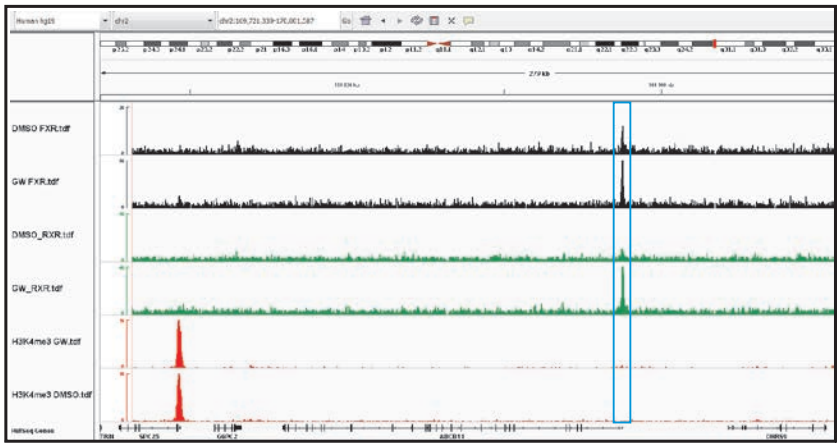

Supplemental Figure 20- Lien et al

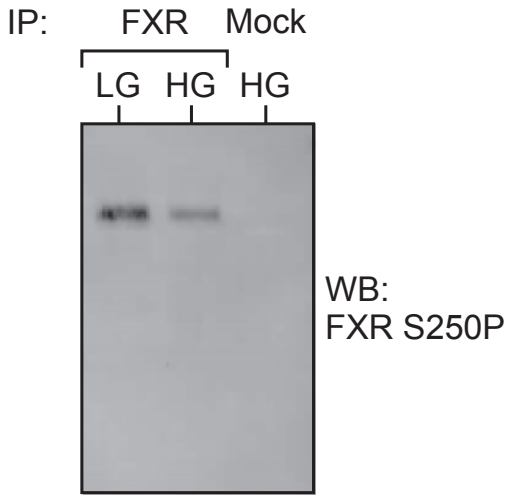

Supplemental Figure 21- Lien et al